Journal for ImmunoTherapy of Cancer

Immune cell and tumor cell-derived CXCL10 is indicative of immunotherapy response in metastatic melanoma

Robin Reschke ,[1] Jovian Yu,[2] Blake A Flood,[1] Emily F Higgs,[1] Ken Hatogai,[1,2] Thomas F Gajewski[1,2]

To cite: Reschke R, Yu J, Flood BA, *et al*. Immune cell and tumor cell-derived CXCL10 is indicative of immunotherapy response in metastatic melanoma. *Journal for ImmunoTherapy of Cancer* 2021;**9**:e003521. doi:10.1136/jitc-2021-003521

► Additional supplemental material is published online only. To view, please visit the journal online (http://dx.doi.org/10.1136/jitc-2021-003521).

Accepted 11 August 2021

[1]Department of Pathology, University of Chicago, Chicago, Illinois, USA
[2]Department of Medicine, Section of Hematology/Oncology, University of Chicago, Chicago, Illinois, USA

Correspondence to
Professor Thomas F Gajewski; tgajewsk@medicine.bsd.uchicago.edu

ABSTRACT

A T cell-inflamed tumor microenvironment is characterized by the accumulation and local activation of CD8$^+$ T cells and Bat3-lineage dendritic cells, which together are associated with clinical response to anti-programmed cell death protein 1 (anti-PD-1)-based immunotherapy. Preclinical models have demonstrated a crucial role for the chemokine CXCL10 in the recruitment of effector CD8$^+$ T cells into the tumor site, and a chemokine gene signature is also seen in T cell-inflamed tumors from patients. However, the cellular source of CXCL10 in human solid tumors is not known. To identify the cellular source of CXCL10 we analyzed 22 pretreatment biopsy samples of melanoma metastases from patients who subsequently underwent checkpoint blockade immunotherapy. We stained for CD45$^+$ and Sox10$^+$ cells with multiparameter immunofluorescence staining, and RNA in situ hybridization technology was used in concert to identify CXCL10 transcripts. The results were correlated with the expression levels of CXCL10 transcripts from bulk RNA sequencing and the best overall response to immune checkpoint inhibition (anti-PD-1 alone or with anti-CTLA-4) in the same patients. We identified CD45$^+$ cells as the major cellular source for CXCL10 in human melanoma metastases, with additional CXCL10 production seen by Sox10$^+$ cells. Up to 90% of CD45$^+$ cells and up to 69% of Sox10$^+$ cells produced CXCL10 transcripts. The CXCL10 staining result was consistent with the level of CXCL10 expression determined by bulk RNA sequencing. The percentages of CD45$^+$ CXCL10$^+$ cells and Sox10$^+$ CXCL10$^+$ cells independently predicted response ($p<0.001$). The average number of transcripts per cell correlated with the CD45$^+$ cell infiltrate ($R=0.37$). Immune cells and melanoma cells produce CXCL10 in human melanoma metastases. Intratumoral CXCL10 is a positive prognostic factor for response to immunotherapy, and the RNAscope technique is achievable using paraffin tissue. Strategies that support effector T cell recruitment via induction of CXCL10 should be considered as a mechanism-based intervention to expand immunotherapy efficacy.

INTRODUCTION

Immunotherapy strategies have revolutionized cancer care, particularly with the demonstrated efficacy and Food and Drug Administration approval of anti-CTLA-4 and anti-PD-1/PD-L1 antibodies. Patients with metastatic melanoma receive either monotherapy with an anti-PD-1 monoclonal antibody (mAb) or a combination of checkpoint blockade with anti-CTLA-4 and anti-PD-1 as first-line treatment.[1 2] However, a majority of patients with metastatic melanoma still does not experience clinical benefit,[3] and the reasons for immunotherapy resistance are only beginning to be understood. One major predictive factor for response to immunotherapy is the presence of cytotoxic CD8$^+$ T cells and a T cell-inflamed gene expression profile in the tumor microenvironment.[4–6] A pretreatment interferon (IFN)-γ-related transcriptional profile has been shown to enrich for responders to anti-PD1-therapy.[7] Therefore, migration and trafficking of CD8$^+$ effector T cells into the tumor microenvironment is an essential step for immunotherapy efficacy. In general, T cell entry into inflamed tissues involves adhesion and transmigration across vascular endothelial cells, along with sensing of chemokine gradients for directional trafficking. Preclinical studies have demonstrated that recruitment of activated CD8$^+$ T cells into tumor sites is driven predominantly by the chemokines C-X-C motif chemokine ligand 9 (CXCL9) and CXCL10, with CXCL10 being the more abundantly expressed entity. These chemokines engage the corresponding chemokine receptor CXCR3 which is expressed on activated CD8$^+$ T cells and other immune cells.[4 8–10] Increased levels of CXCL10 were associated with tumor infiltration with effector CD4$^+$, CD8$^+$, and natural killer cells which coincided with reduced tumor growth.[11–13] In a melanoma model, CXCR3 knock out mice showed significantly fewer CD8$^+$ T cells within the tumor microenvironment and failed to respond to anti-PD-1 therapy compared with wild-type mice.[14] Human melanoma metastases having a T cell-inflamed phenotype also show expression of

CXCL9 and CXCL10 by bulk RNAseq analysis, as well as the related human-expressed chemokine CXCL11.[4] It has been presumed that the local production of these chemokines within tumor sites is a major mechanism of effector T cell recruitment into human tumors as well, and for immunotherapy efficacy in the clinic.

A critical mechanistic question is the cellular origin of the chemokines for T cell entry into the tumor microenvironment, which is important as it is such an important rate-limiting step for the effector phase of the antitumor immune response. In a genetically engineered mouse model of melanoma, dendritic cells driven by the basic leucine zipper transcription factor ATF-like 3 dendritic cells (Batf3-lineage DCs) were found to be a major functionally important source of CXCL9 and CXCL10.[9] Elimination of Batf3-lineage DCs prevented trafficking of $CD8^+$ T cells into tumor sites and was associated with failed efficacy of multiple immunotherapy modalities. However, other cell types are also capable of CXCL9/10 production. During the early characterization of a chemokine gene signature in melanoma, occasional melanoma tumor cell lines were found to produce CXCL10 in vitro.[4] However, within the human melanoma microenvironment in vivo, the cellular source of CXCL9 and CXCL10 remains unknown. With this knowledge gap in mind, we developed a strategy to integrate multiparameter immunofluorescence staining with RNA in situ hybridization (RISH) technology, to begin to understand the cellular source of key chemokines within T cell-inflamed tumors. We focused on CXCL10 as it is more abundantly expressed and likely is more functionally important. As the major question is whether immune cells or cancer cells are the predominant source, we utilized anti-CD45 staining as well as anti-Sox10 to mark melanoma cells. We found that $CD45^+$ cells are the major source of CXCL10 messenger RNA, with some transcripts being detected in $Sox10^+$ cells. Transcript signals detected by RISH correlated with bulk RNAseq results, which indicates association with the overall T cell-inflamed gene signature. As these samples were obtained at baseline prior to checkpoint blockade therapy, clinical outcomes were investigated. Indeed, higher percentages of immune cells producing CXCL10 correlated with response to checkpoint blockade. Our results argue that increased production of CXCL10 in the tumor microenvironment is a positive predictive factor for response to immunotherapy, prompting considerations of therapeutic strategies to promote inflammatory signals that include CXCL10 to expand immunotherapy efficacy.

MATERIALS AND METHODS

Patient samples

For the in situ multiparameter staining, tissue sections from 22 patients with advanced metastatic melanoma being treated with anti-PD-1-based immunotherapy were studied retrospectively. The samples were collected before patients commenced immunotherapy with anti-PD-1 (either nivolumab or pembrolizumab) alone or in combination with anti-CTLA-4 (ipilimumab) for metastatic melanoma. Four patients received combination treatment with anti-PD-1 and anti-CTLA-4. All patients were previously treatment-naïve for anti-PD-1 blockade. One patient had prior checkpoint blockade with anti-CTLA-4 in the adjuvant setting 3 months prior to starting the combination treatment. The response group was categorized as partial response (PR) and complete response (CR), whereas the non-response group included stable disease (SD) and progressive disease (PD). CR, PR, SD, and PD were determined with Response Evaluation Criteria In Solid Tumors (RECIST) criteria after a minimum of 6 months.

RNA-in situ hybridization technology combined with immunofluorescence staining for protein

Co-detection of RNA and protein antigens in the same samples was achieved by RISH using the RNAscope Multiplex Fluorescent Reagent Kit v2, together with antibody-based immunofluorescence staining. Positive (POLRA2, PPIB, UBC) and negative RNA probe (dapB) controls, CXCL10 RNA probe (HS-CXCL10, Catalog Nr. 311851) and CD45 antibody (Leukocyte Common Antigen Cocktail: PD7/26/16 and 2B11, BioCare Medical) and Sox10 (MAB2864, Novus Biologicals/Bio-Techne) were tested individually on primary melanoma and metastatic melanoma tissue. After the successful staining of the individual targets, all markers were stained together with the co-detection protocol and optimized on metastatic melanoma tissue. The manufacturer's integrated co-detection protocol was followed (Advanced Cell Diagnostics, ACD). Formalin-fixed paraffin-embedded metastatic melanoma tissue sections were baked for 30 min at 60°C in an ACD oven (HybEZ Oven). After the baking they were deparaffinized by submerging in xylenes for 5 mins twice, rehydrated in 100% ethanol for 1 min twice, air dried, treated with RNAscope hydrogen peroxide for 10 min, and rinsed with distilled water. A TintoRetriever Pressure cooker (Bio SB) was used to perform Target retrieval with 1× Co-Detection Target Retrieval (ACD) solution at 98°C–102°C for 15 min. Slides were rinsed in distilled water and 1× Phosphate-Buffered Saline Tween (PBST) buffer. For the blocking step Co-Detection antibody diluent (ACD) was used. Tissue sections were incubated with anti-Sox10 antibody overnight at 4°C. Subsequently, they were washed in PBST buffer, incubated in 10% Neutral Buffered Formalin for 30 min at room temperature, and washed in PBST. Tissue sections were treated with RNAscope Protease plus at 40°C for 15 min and rinsed in distilled water. RISH was performed in accordance with the RNAscope assay protocol. Briefly, sections were incubated with CXCL10 RNA probe and hybridized at 40°C for 2 hours. The RNAscope Multiplex FL v2 AMP reagents were used to perform signal amplification in the following order: AMP1 (30 min, 40°C), AMP2 (30 min, 40°C), and AMP3 (15 min, 40°C). Horseradish peroxidase (HRP) signal was developed according to manufacture protocol.

Fluorescent labeling of the CXCL10 RNA probes was performed using OPAL 570 dye (Akoya Biosciences). The Sox10 primary antibody was detected with HRP-conjugated secondary antibody (Opal Polymer HRP Ms+Rb, PerkinElmer) and Opal 690 dye. Subsequent staining on the same sections was performed with an antibody against CD45 and detected with (HRP)-conjugated secondary antibody and Opal 520 dye. Tissue sections were incubated with 4′,6-diamidino-2-phenylindole (DAPI) solution for 5 min at room temperature. Finally, they were mounted in ProLong Diamond Antifade Mountant (Invitrogen). Scanning of the slides was performed using the Vectra Polaris imaging platform and Phenochart software (PerkinElmer). For each tissue section 10–45 representative regions of interest (ROI) for each tissue section were acquired at 40× magnification as multispectral images. A supervised machine learning algorithm within the inForm V.2.3 software (PerkinElmer), which assigned trained phenotypes and cartesian coordinates to cells was used to perform image analysis and cell phenotyping. CellProfiler V.4.1.3 was used to perform spot counting of the CXCL RNA transcripts.

RNA sequencing and tumor inflammation signature

RNA sequencing was performed by the University of Chicago Genomics Core facility using the Illumina HiSeq platform. Pseudoalignment was performed using Kallisto. All submitted samples passed quality control using the R package FastQC. Raw read counts were processed by TMM normalization followed by log2 transformation. Tumor inflammation signatures (TIS) were calculated as the median of normalized log2-expression of the following 18 genes: PSMB10, HLA-DQA1, HLA-DRB1, CMKLR1, HLA-E, NKG7, CD8A, CCL5, CXCL9, CD27, CXCR6, IDO1, STAT1, TIGIT, LAG3, CD274, PDCD1LG2, CD276.[15]

Statistical analysis

Statistics were done using R V.4.0.5, and the tidyverse, patchwork, phenoptr, ggsignif, ggpmisc, ggpubr, and scales packages. Boxplots show the medians (middle line) and the first and third quartiles (upper and lower bounds of the boxes). Significance of comparisons from boxplots were determined by Mann-Whitney-Wilcoxon test and significance is expressed as p values, shown as asterisk (*, p≤0.05; **, p≤0.01; ***, p≤0.001). Scatter plots show linear regression lines with associated CIs in dark gray. Full modeled equation with x coefficient and intercept values displayed in upper left of each scatter plot with R2 correlation coefficient of regression model.

RESULTS

For each sample, the tumor microenvironment was visually dissected into two main cell populations with immunofluorescence staining: $CD45^+$ immune cells versus $Sox10^+$ tumor cells. By staining for cells that express the leukocyte common antigen (CD45), a broad assessment of immune cells was achieved including myeloid and lymphoid cells. The transcription factor Sry-related HMg-Box gene 10 (Sox10) was used to stain the nuclei of melanoma cells (figure 1A). Simultaneously, CXCL10 RNA transcripts were stained with RISH in order to see the distribution of transcripts within immune and tumor cells (figure 1B). A 40× magnified scanning protocol allowed for precise detection of single spots. One immunofluorescent spot is thought to be representative of one RNA transcript.[16] An average of 58% of $CD45^+$ cells (10%–90%) expressed CXCL10 transcripts. However, an average of 38% of $Sox10^+$ cells (1%–69%) also demonstrated CXCL10 production, with only a small proportion of DAPI-only positive cells producing CXCL10. The percentage of all $CXCL10^+$ cells including stromal cells (nuclei DAPI positive) was correlated with bulk RNA sequencing results (figure 1C). RISH results for percentage of $CXCL10^+$ cells correlated significantly with transcript levels of CXCL10 in bulk RNAseq.

Next, the relationship with clinical response was investigated (figure 1D). The median percentage of $CXCL10^+$ cells in the tumor microenvironment of melanoma metastases was significantly higher in patients who responded to subsequent checkpoint inhibition (CR >PR>SD>PD). Pairwise comparisons showed the strongest difference between patients with progressive disease and patients with partial response ($p<0.01$). Comparisons of percentages of $CXCL10^+$ cells between patients with PD and CR and between patients with SD and PR were also significant ($p<0.1$). When classified into response (PR +CR) and non-response (SD +PD) with 11 patients in each group the biological difference became more apparent (figure 2). Percentage of all cells producing CXCL10, percentage of $Sox10^+$ $CXCL10^+$ cells and percentage of $CD45^+$ $CXCL10^+$ cells were independently capable of predicting response to checkpoint blockade ($p<0.001$) (figure 2A,B). The response group showed not only significantly more CXCL10 transcripts but also on average more $CD45^+$ cells (figure 2C). Generally, $CD45^+$ cells were the predominant cell population for CXCL10 production which also reflects in higher mean fluorescence intensity per cell count despite bigger melanoma cell clusters in most cases (figure 2D). Counting the number of spots per cell revealed that the vast majority of $CXCL10^+$ immune or tumor cells only produced one or two transcripts per cell (online supplemental figure 1). However, the mean number of spots per cell in each ROI correlated weakly with CD45 infiltrate (online supplemental figure 2). The percentages of $CD45^+$ $CXCL10^+$ cells correlated weakly with $Sox10^+$ $CXCL10^+$ cells on a per patient basis (online supplemental figure 3), arguing for a relationship between these two chemokine-producing cell populations. In order to test if there was a correlation between CXCL10 expression level and a general tumor inflamed phenotype, the percentage of all $CXCL10^+$ cells was correlated with a published TIS.[15] The TIS consists of the following 18 genes: PSMB10, HLA-DQA1, HLA-DRB1, CMKLR1, HLA-E, NKG7, CD8A, CCL5, CXCL9, CD27,

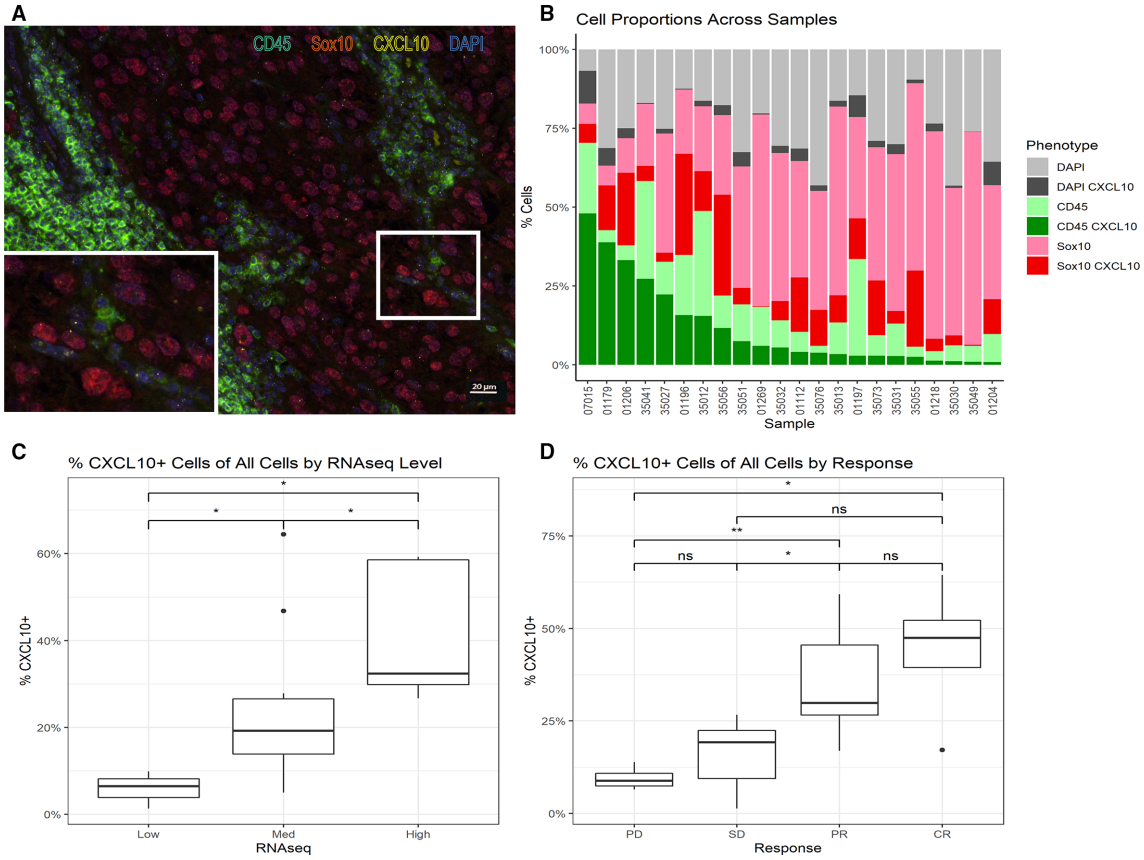

Figure 1 (A) Representative regions of interest of patient 35041: RNA in situ hybridization staining for CXCL10 RNA (yellow spots), immunofluorescence staining of CD45$^+$ cells (green), Sox10$^+$ cells (red) and DAPI counterstain (blue). (B) Cell proportions across all 22 samples on a per patient basis: Percentages of CD45$^+$ cells (light green), CD45$^+$ CXCL10$^+$ cells (dark green), Sox10$^+$ cells (pink), Sox10$^+$ CXCL10$^+$ cells (red), DAPI (light gray), and DAPI CXCL10$^+$ (dark gray). (C) Percentage of all CXCL10 positive cells on a per patient basis correlated to RNA sequencing results for CXCL10 transcripts divided into low 0–3.28, medium 3.28–6.56 and high 6.56–9.84 (all RNAseq scores log2-transformed). (D) Percentage of all CXCL10 positive cells on a per patient basis correlated to immunotherapy response groups (PD, SD, PR ad CR). (**=p <0.01, *=p <0.05). CR, complete response; PD, progressive disease; PR, partial response; SD, stable disease.

CXCR6, IDO1, STAT1, TIGIT, LAG3, CD274, PDCD1LG2, CD276. These genes are associated with antigen presentation, chemokine expression, cytotoxic activity, and adaptive immune resistance.[15] The TIS correlated with response to anti-PD1 therapy in melanoma and has been used in various cancer types to assess the adaptive immunity within the tumor microenvironment.[15 17] In particular, patient samples with high TIS also expressed high levels of CXCL10 transcripts (online supplemental figure 4) which indicates a correlation between CXCL10 expression in melanoma and an inflamed phenotype with tumor-infiltrating leukocytes.

When comparing ROIs of patients with response to non-responding patients, these statistical differences can also be seen visually. In figure 3, one exemplary ROI of a response patient is depicted with the complete panel (figure 3A) and individual fluorescence channels turned on (figure 3B–D). When magnified, high expression levels of CXCL10 transcripts are shown with yellow spots particularly in the immune cell compartment. As a contrasting image, the patient represented in figure 4 who later progressed has significantly fewer CXCL10 transcripts. In the magnified area of the chosen ROI, 10 total CXCL10 spots can be seen, with a much diminished CD45$^+$ infiltrate.

DISCUSSION

Chemokines play a crucial role in recruiting and potentiating the effect of immune cells in the tumor microenvironment. A major mechanism of resistance to therapy with checkpoint blockade is exclusion of cytotoxic CD8$^+$ T cells from the tumor. These non-inflamed tumors progress despite anti-PD-1 therapy, and efficacy of anti-PD-1 is enriched in patients with T cell-inflamed tumors.[5] Preclinical models have demonstrated that CXCL10 is a critical chemokine for the recruitment of CD8$^+$ T cells into melanoma lesions.[9] Batf3-lineage DCs have been identified as a predominant source of CXCL10 in mice.[9] Gene expression profiling of human melanoma metastases has also revealed that higher expression levels of CXCL10 is associated with an influx of CD8$^+$ T cells.[4] Furthermore, some human melanoma cell lines (such

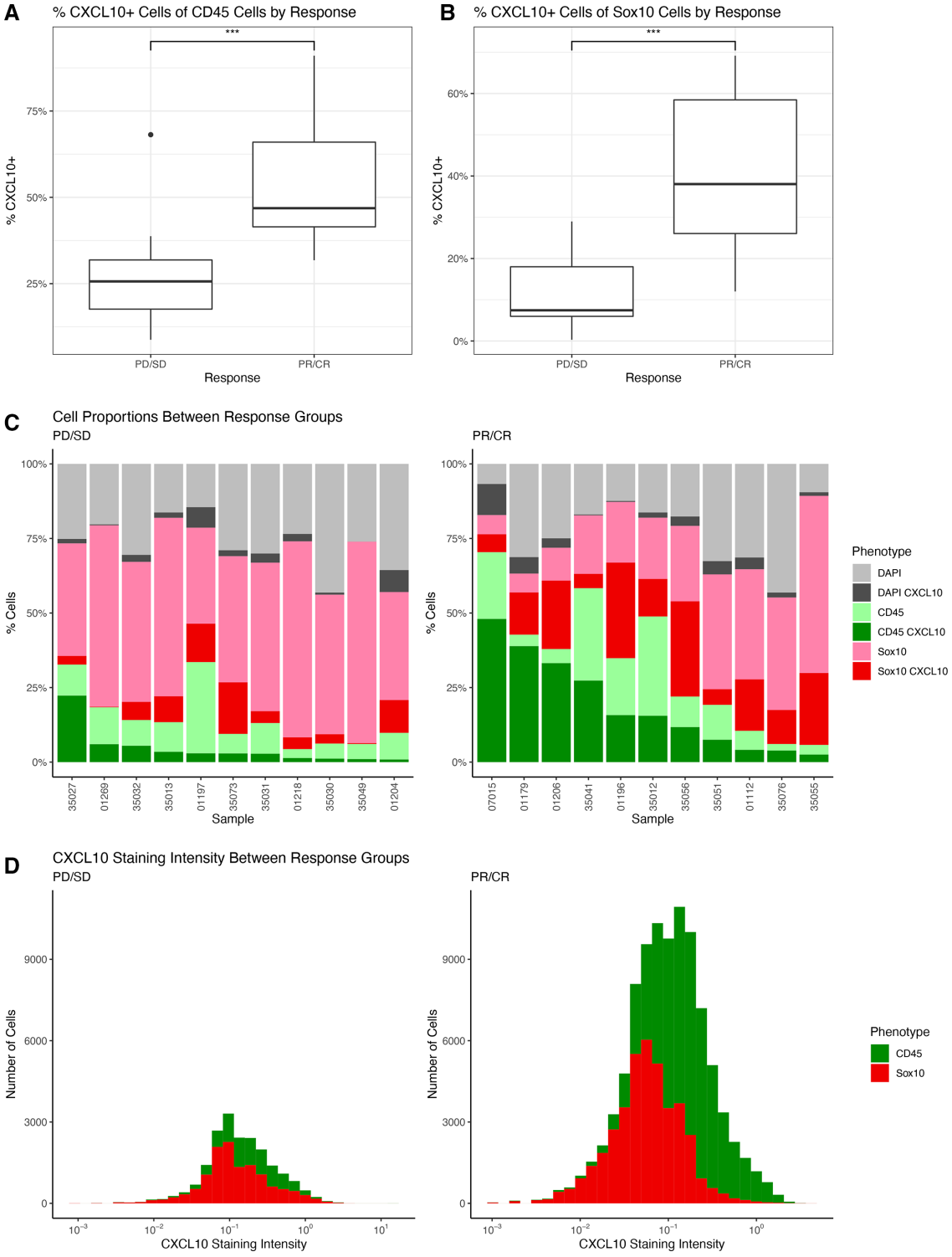

Figure 2 (A) Percentage of CD45$^+$ CXCL10$^+$ cells on a per patient basis correlated with response divided into two groups (PD/SD and PR/CR). (B) Percentage of Sox10$^+$ CXCL10$^+$ cells on a per patient basis correlated with response divided into two groups (PD/SD and PR/CR). (C) Cell proportions across samples divided into two response groups (PD/SD and PR/CR): Percentages of CD45$^+$ cells (light green), CD45$^+$ CXCL10$^+$ cells (dark green), Sox10$^+$ cells (pink), Sox10$^+$ CXCL10$^+$ cells (red), DAPI (light gray), and DAPI CXCL10$^+$ (dark gray). (***=p <0.001). (D) Cell count of CD45$^+$ CXCL10$^+$ cells (green) and Sox10$^+$ CXCL10$^+$ cells (red) cells correlated to staining intensity of CXCL10 within these phenotypes measured by mean fluorescence intensity (on a per cell basis). CR, complete response; PD, progressive disease; PR, partial response; SD, stable disease.

as M537 cells) have been demonstrated to be capable of producing CXCL10, which was associated with the recruitment of human primed CD8$^+$ effector T cells in vitro and in vivo.[4] Single-cell RNA sequencing analysis of two melanoma, one head and neck and one lung cancer data set found that macrophages

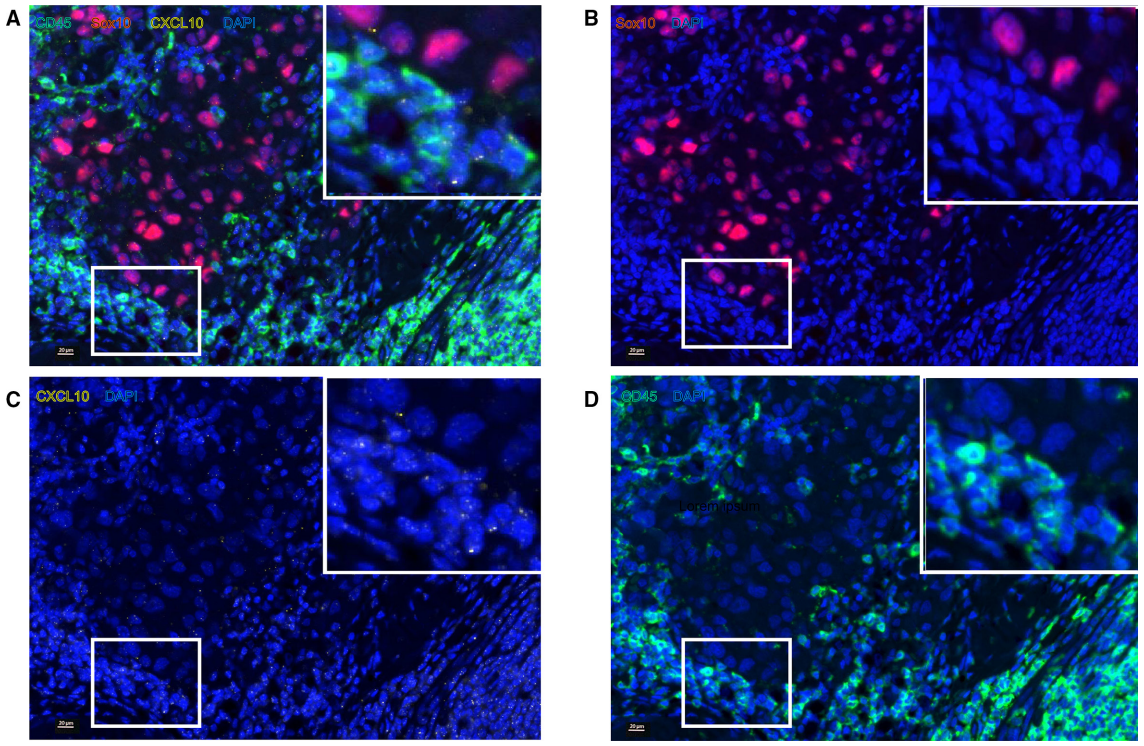

Figure 3 Representative regions of interest of the response patient 01179 (partial response). (A) Complete panel consisting of CD45$^+$ cells (green), Sox10$^+$ cells (red), CXCL10 transcripts (yellow spots), DAPI nuclear counterstain (blue), (B) Sox10$^+$ cells (red), DAPI (blue), (C) CXCL10 RNA (yellow spots), DAPI (blue), (D) CD45$^+$ cells (green), DAPI (blue).

were the predominant source of CXCL10 in human cancers.[18] A noteworthy but lower expression was found in dendritic cells such as the CLEC9A$^+$ cDC1s.[18] The differential gene expression analysis of the one melanoma data set that was correlated with response to immunotherapy revealed higher expression of CXCL10 in macrophages of responding patients.[18 19] The findings of our current study, namely that that

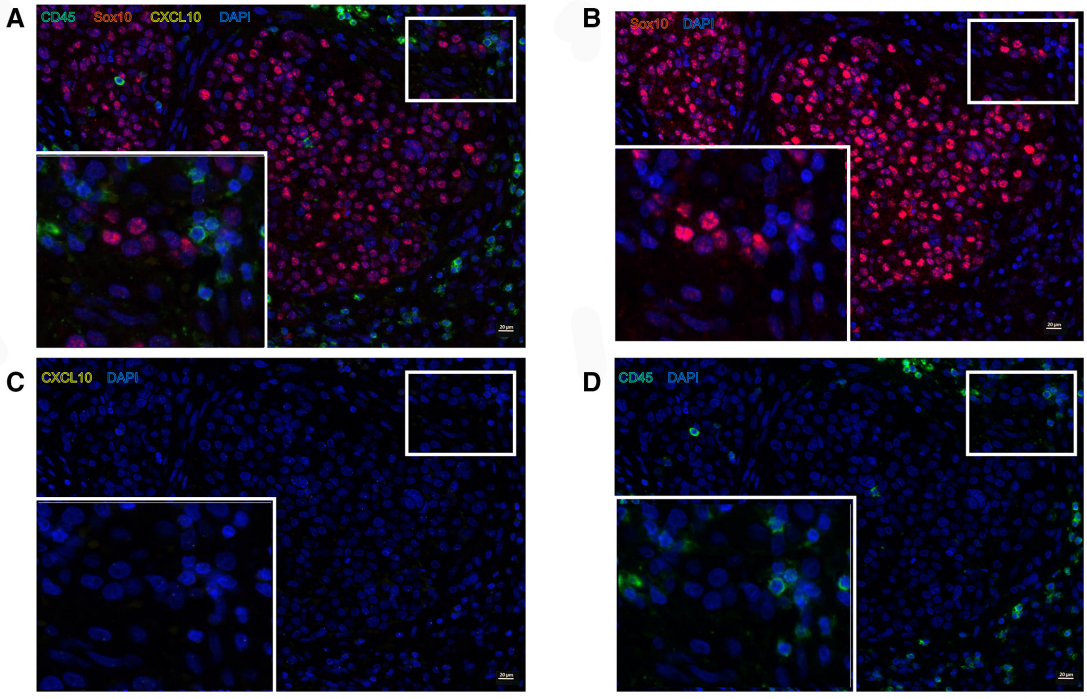

Figure 4 Representative regions of interest of a non-response patient 35 031 (progressive disease). (A) Complete panel consisting of CD45$^+$ cells (green), Sox10$^+$ cells (red), CXCL10 transcripts (yellow spots), DAPI nuclear counterstain (blue), (B) Sox10$^+$ cells (red), DAPI (blue), (C) CXCL10 RNA (yellow spots), DAPI (blue), (D) CD45$^+$ cells (green), DAPI (blue).

CD45$^+$ immune cells are the predominant source of CXCL10, are in agreement with that report. However, by examining entire paraffin-embedded tissue sections rather than sorted cell populations, we were able to identify Sox10$^+$ tumor cells as a second source of CXCL10. Percentages of both cell populations producing CXCL10 (CD45$^+$ CXCL10$^+$ and Sox10$^+$ CXCL10$^+$) were able to predict clinical response, arguing overall for an important predictive role of CXCL10 in the tumor microenvironment. CXCL9 and CXCL11 also bind to CXCR3 in human immune cells. Baseline relative expression levels of CXCL9, CXCL10 and CXCL11 were higher in patients with melanoma who responded to anti-PD-1 measured by bulk RNAseq,[18] although in our samples CXCL10 showed the highest relative expression level and gave reproducible RNA staining results we cannot exclude a predictive value of the other CXCR3-ligands. Because CXCL10 production can be induced by IFN-γ, it seems likely that tumors which contain activated CD8$^+$ T cells end up with secondary production of CXCL10 by melanoma cells in response to secreted IFN-γ. However, de novo production of CXCL10 by tumor cells cannot be excluded. Using recombinant viral vectors or engineered stem cells to induce CXCL10 expression led to reduced tumor growth and fewer metastases in multiple in vivo and in vitro melanoma models.[11 20 21] Innate immune activators and oncolytic viruses also could be considered as therapeutic interventions to promote greater CXCL10 production in vivo.

CONCLUSION

CXCL10 is a key chemokine that is responsible for recruitment of tumor antigen specific CD8$^+$ T cells in the tumor microenvironment. It can be produced by immune cells, that is, macrophages and DCs, but also to a lesser extent by melanoma cells. CXCL10 expression is strongly associated with response to immune checkpoint inhibition and can predict response independent of the immune cell infiltrate. The RNAscope technology is useful as it can be applied to paraffin-embedded tissues. Strategies to induce or potentiate CXCL10 production in the tumor microenvironment could be considered as an approach to expand checkpoint blockade efficacy.

Correction notice This article has been corrected since it was first published. Middle initial has been added to author name 'Blake A Flood'.

Twitter Jovian Yu @jovianyu

Contributors RR and TFG conception and design; RR development of methodology and acquisition of data; KH helped with microscopy; RR, JY, BAF, and EFH analysis; RR, JY, and BAF interpretation of data; RR writing of the manuscript; TFG review and revision of the manuscript; TFG study supervision. All authors approved the final version of the manuscript, including the authorship list.

Funding RR was funded by the German Research foundation (DFG RE 4468/1–1), JY was funded by National Institutes of Health Basic Research Training in Medical Oncology grant (T32 CA009566-33), EFH was funded by National Institutes of Health F30CA250255. KH was funded by Japan Cancer Society Relay for Life Awards (2017), Japan Society for the Promotion of Science Overseas Research Fellowships (2019), TFG was funded by National Institutes of Health (R35CA210098).

Competing interests None declared.

Patient consent for publication Not required.

Ethics approval The study was approved by the University of Chicago Institutional Review Board (IRB protocol 15–0837).

Provenance and peer review Not commissioned; externally peer reviewed.

Data availability statement Data are available upon reasonable request. Raw data available upon reasonable request.

ORCID iD

Robin Reschke http://orcid.org/0000-0002-2850-2526

REFERENCES

1 Postow MA, Chesney J, Pavlick AC, *et al*. Nivolumab and ipilimumab versus ipilimumab in untreated melanoma. *N Engl J Med* 2015;372:2006–17.
2 Ribas A, Puzanov I, Dummer R, *et al*. Pembrolizumab versus investigator-choice chemotherapy for ipilimumab-refractory melanoma (KEYNOTE-002): a randomised, controlled, phase 2 trial. *Lancet Oncol* 2015;16:908–18.
3 Larkin J, Chiarion-Sileni V, Gonzalez R, *et al*. Five-year survival with combined nivolumab and ipilimumab in advanced melanoma. *N Engl J Med* 2019;381:1535–46.
4 Harlin H, Meng Y, Peterson AC, *et al*. Chemokine expression in melanoma metastases associated with CD8$^+$ T-cell recruitment. *Cancer Res* 2009;69:3077–85.
5 Tumeh PC, Harview CL, Yearley JH, *et al*. PD-1 blockade induces responses by inhibiting adaptive immune resistance. *Nature* 2014;515:568–71.
6 Chen P-L, Roh W, Reuben A, *et al*. Analysis of immune signatures in longitudinal tumor samples yields insight into biomarkers of response and mechanisms of resistance to immune checkpoint blockade. *Cancer Discov* 2016;6:827–37.
7 Ayers M, Lunceford J, Nebozhyn M, *et al*. IFN-γ-related mRNA profile predicts clinical response to PD-1 blockade. *J Clin Invest* 2017;127:2930–40.
8 Mikucki ME, Fisher DT, Matsuzaki J, *et al*. Non-redundant requirement for CXCR3 signalling during tumoricidal T-cell trafficking across tumour vascular checkpoints. *Nat Commun* 2015;6:7458.
9 Spranger S, Dai D, Horton B, *et al*. Tumor-Residing Batf3 dendritic cells are required for effector T cell trafficking and adoptive T cell therapy. *Cancer Cell* 2017;31:711–23.
10 Bagheri H, Pourhanifeh MH, Derakhshan M, *et al*. CXCL-10: a new candidate for melanoma therapy? *Cell Oncol* 2020;43:353–65.
11 Antonicelli F, Lorin J, Kurdykowski S. CXCL10 reduces melanoma proliferation and invasiveness in vitro and in vivo: CXCL10 and melanoma progression. *Br J Dermatol* 2011;164:720–8.
12 Barash U, Zohar Y, Wildbaum G, *et al*. Heparanase enhances myeloma progression via CXCL10 downregulation. *Leukemia* 2014;28:2178–87.
13 Arenberg DA, White ES, Burdick MD, *et al*. Improved survival in tumor-bearing SCID mice treated with interferon-gamma-inducible protein 10 (IP-10/CXCL10). *Cancer Immunol Immunother* 2001;50:533–8.

14 Chheda ZS, Sharma RK, Jala VR, *et al*. Chemoattractant receptors BLT1 and CXCR3 regulate antitumor immunity by facilitating $CD8^+$ T cell migration into tumors. *J Immunol* 2016;197:2016–26.
15 Danaher P, Warren S, Lu R, *et al*. Pan-cancer adaptive immune resistance as defined by the tumor inflammation signature (TIS): results from the cancer genome atlas (TCGA). *J Immunother Cancer* 2018;6:63.
16 Wang F, Flanagan J, Su N, *et al*. RNAscope. *J Mol Diagn* 2012;14:22–9.
17 Ayers M, Lunceford J, Nebozhyn M, *et al*. Relationship between immune gene signatures and clinical response to PD-1 blockade with pembrolizumab (MK-3475) in patients with advanced solid tumors. *J Immunother Cancer* 2015;3:P80.
18 House IG, Savas P, Lai J, *et al*. Macrophage-Derived CXCL9 and CXCL10 are required for antitumor immune responses following immune checkpoint blockade. *Clin Cancer Res* 2020;26:487–504.
19 Sade-Feldman M, Yizhak K, Bjorgaard SL, *et al*. Defining T cell states associated with response to checkpoint immunotherapy in melanoma. *Cell* 2018;175:998–1013.
20 Feldman AL, Friedl J, Lans TE, *et al*. Retroviral gene transfer of interferon-inducible protein 10 inhibits growth of human melanoma xenografts. *Int J Cancer* 2002;99:149–53.
21 Mirzaei H, Salehi H, Oskuee RK, *et al*. The therapeutic potential of human adipose-derived mesenchymal stem cells producing CXCL10 in a mouse melanoma lung metastasis model. *Cancer Lett* 2018;419:30–9.